

Simple Preparation of High-Quality Graphene Flakes without Oxidation Using Potassium Salts

Jiyoung Kwon, Sun Hwa Lee, Kwang-Hyun Park, Dong-Hwa Seo, Jinsup Lee, Byung-Seon Kong, Kisuk Kang,* and Seokwoo Jeon*

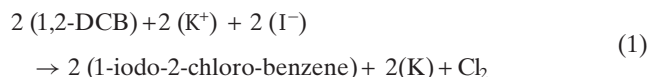
Graphene is a 2D sheet of sp^2 -hybridized carbon with interesting properties, including exceptionally high thermal/electrical conductivity, surface area, and mechanical strength.^[1–5] Many fabrication methods have been proposed to obtain graphene so as to utilize these interesting properties. The approaches to fabricate graphene can be roughly categorized into two classes: i) top-down exfoliation of multilayer graphene or graphite by breaking π -bonding between carbon atoms,^[6–10] and ii) bottom-up formation of sp^2 -bonding between carbon atoms in a monolayer.^[11–16] Mechanical and chemical exfoliation methods fall into the first category, while chemical vapor deposition (CVD) and epitaxial growth from silicon carbide (SiC) belong to the second. Flake-types of graphene promise potential applications in the fields of transparent electrodes, energy storage, electromagnetic (EM) shields, etc.^[17–19] Dispersed graphene flakes are mostly produced by a chemical exfoliation method, through chemical oxidation and reduction, known as Hummers' method.^[20] Hummers' method is a low-cost process applicable to mass production. However, the quality of the achieved graphene is often below desired levels, mainly due to the presence of residual oxygen, even after a sufficient reduction process.^[21] Here, we firstly introduce a new method to acquire high-quality graphene flakes by simply using metal salts without oxidation.

Graphite intercalation compounds (GICs) are typically formed by the insertion of atomic or molecular species, called intercalants, between layers in a graphite host. The formation of GICs has been an active field of research especially in relation to lithium ion batteries because graphite can store a large amount

of Li in its crystal structure, and therefore serve as anodes with high energy density.^[22,23] Alkali metal atoms (Li, Na, K, Rb, Cs) and alkali earth metal atoms (Be, Mg, Ca, Sr, Ba, Ra) are well-known intercalants of graphite. Generally, when the ionization potential of intercalants is lower than the electron affinity of graphite (4.6 eV), intercalation occurs spontaneously.^[24] While the intercalation kinetics is dependent on the ionic size and the valence of the intercalants, potassium, rubidium, and cesium can intercalate into graphite at relatively low temperatures (<300 °C) and ambient pressure.^[25] When they form GICs, the interlayer distance of graphite increases above 0.5 nm (K-GICs: 0.53 nm, Rb-GICs: 0.56 nm, Cs-GICs: 0.59 nm), which is about 1.5 times larger than that of Li-GICs and approaches the value of graphite oxide.^[26] The interlayer distance of GICs can surpass 0.5 nm when co-intercalation simultaneously involves both metals and organic molecules.^[27] In this work, taking into consideration availability and cost-effectiveness, we use K-GICs to produce few-layer graphene flakes.

In most previous reports on alkali-metal-GICs, reactive alkali metal has been directly used as a source to form GICs.^[6,25] However, because alkali metals are typically unstable in ambient conditions and even become explosive, the graphene fabrication process becomes more complicated, and safety is a greater concern. The easy surface oxidation of alkali metals also makes the control of oxygen content difficult. This adds considerable complexity in the preparation of GIC and, therefore, increases the fabrication cost. Here, we show that the use of salts is a promising alternative. Although alkali metal salts have a strong catalytic influence upon the reactions of carbonaceous materials with oxygen, carbon dioxide, and water vapor at elevated temperatures,^[28,29] the graphite source in the proposed method undergoes a mild intercalation process below 500 °C. The formed graphite intercalation compound, without further degradation or reaction, transforms into graphene flakes without oxidation. The process is fully mass producible, and the graphene flakes obtained from the GICs have better material properties because the overall process excludes the introduction of oxygen.

Figure 1 shows a schematic illustration of the overall process to obtain graphene flakes in a pressured vessel (Parr 4651). First, the following chemical reaction (Equation 1) occurs between 1,2-dichlorobenzene (1,2-DCB) and potassium iodide at 300 °C in an encapsulated system for 10 h.



J. Kwon, Dr. S. H. Lee, K. H. Park, J. Lee, Prof. S. Jeon
Department of Materials Science and Engineering
Institute for Nanocentury
Korea Advanced Institute of Science and Technology (KAIST)
Daejeon, 305–701, Republic of Korea
E-mail: jeon39@kaist.ac

Prof. K. Kang
Department of Materials Science and Engineering
Institute for Eco-Energy
Korea Advanced Institute of Science and Technology (KAIST)
Daejeon, 305–701, Republic of Korea
E-mail: matlgen1@kaist.ac.kr

Dr. D.-H. Seo, Dr. B.-S. Kong
KCC Central Research Institute
Gyunggi-Do, 446–912, Republic of Korea

DOI: 10.1002/sml.201002005

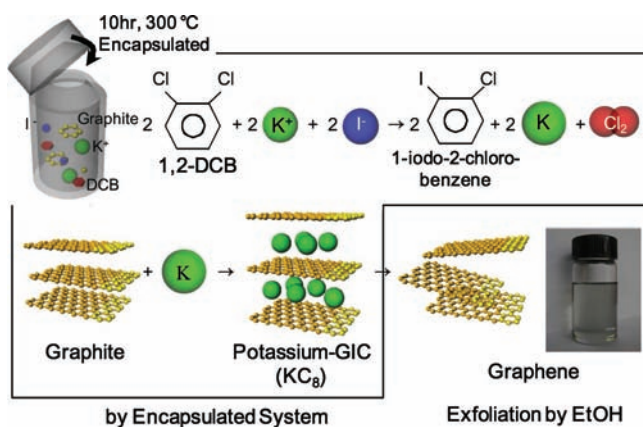
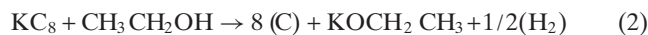


Figure 1. Schematic illustration for forming the graphene. Synthesis of free potassium metal, formation of graphite intercalation compounds, and exfoliation by ethanol are included. Dispersed graphene in 1,2-dichlorobenzene is filtered by vacuum filtration in order to make flexible and transparent graphene sheets.

The formation of 1-iodo-2-chlorobenzene is confirmed by gas chromatography/mass spectroscopy (GC/MS) (Figure S1 in the Supporting Information (SI)). In Figure S1a, a new substance peak at 21.92 min that does not belong to 1,2-DCB is detected. From a mass spectroscopy analysis (Figure S1b) the substance matches well with 1-iodo-2-chlorobenzene. The produced chlorine gas is dissolved in solution after the reaction, and is verified by a pH analysis of the resulting solution. The 1,2-DCB or 1-iodo-2-chloro-benzene solution is initially neutral (Table S1 in the SI). However, when deionized (DI) water is added to the reacted solution, the pH value decreases due to the reaction of $\text{Cl}_2 + \text{H}_2\text{O} \rightarrow \text{HCl} + \text{HClO}$ (Table S2 in the SI). Over time, Cl_2 evaporates from the solution in an open vessel, and the pH value recovers to the original value (~ 6.56) from a value of ~ 3.15 within a day (Table S3 in the SI).

On addition of graphite, the free potassium metal atoms produced from the reaction above start to intercalate into graphene layers and spontaneously form stage I K-GICs at 300°C .^[24,27] The partial exfoliation of graphite in 1,2-DCB further promotes the intercalation of potassium.^[30] A control experiment without the intercalant was performed to help elucidate the role and strong points of the intercalation for generating graphene (Table S4 in the SI). Achieving KC_8 with minimum degradation of the graphitic network is a key step in achieving high-quality graphene flakes. The pressured vessel is transferred to a glove box, and the following procedures are performed in the glove box to minimize oxygen exposure. The generated K-GIC solution is mixed with ethanol and finally produces graphene flakes in a solution from spontaneous reaction between intercalated potassium and the ethanol. Ethanol is an effective exfoliating solvent of K-GIC and removes potassium from graphene, as delineated in Equation 2.^[25]



Residual potassium metal is further removed by sonication.^[25]

Figure 2a and **b** show a high-resolution transmission electron microscopy (HRTEM) image of single-layer graphene and an image of multilayer graphene, respectively. The number of fringes at the edge of the graphene flake is proportional to the number of graphene layers at the given locations. The electron contrast of few-layer graphene significantly depends on the incidence angle, and consequently only relatively small variations become visible in the surface normal.^[31] **Figure 2a** (red arrow) shows a single, observable fringe, but **Figure 2b** (blue arrow) has multiple fringes. Insets are electron diffraction images corresponding to each HRTEM image. An intensity analysis of hexagonal diffraction peaks provides information on both the number of layers and stacking nature. The innermost diffraction spots are from the (100) planes, while second innermost spots are from the (110) planes. According to computational studies of the diffraction intensity (I_{100} and I_{110}) for the Bernal stacking model, the intensity ratio I_{100}/I_{110} of single layer graphene is greater than 1.^[32,33] In contrast, the ratio I_{100}/I_{110} of multilayer graphene is smaller than 0.4.^[32,33] The intensity ratio I_{100}/I_{110} of the inset of **Figure 2a** is 1.2 (see **Figure S2** in the SI). Brighter spots from the 100 planes relative to those from the 110 planes in the inset of **Figure 2a** verify that the sample in **Figure 2a** comprises a single layer. On the contrary, the sample in **Figure 2b** has multilayers, since the 110 spots are brighter than the 100 spots in the inset of **Figure 2b**.

In addition, the shape of the diffraction pattern from the graphene flake, determined by TEM analysis, indirectly verifies that the graphene flake is not oxidized; perfect hexagonal diffraction patterns are clearly shown in the insets.^[34]

Figure 3a and **b** are Raman mapping images showing the number of layers achieved from the shape analysis of **2D** peaks and from the $I_{\text{Dpeak}}/I_{\text{Gpeak}}$ value, I_{Dpeak} and I_{Gpeak} represent the intensity of the **D** and **G** peaks, respectively. Two regions of a graphene sheet, where the size of each region is $5\ \mu\text{m} \times 3\ \mu\text{m}$, are used for the Raman mapping. The film is prepared from a dispersed graphene solution after centrifugation (8000 g, 30 min). Shape analysis of **2D** peaks from

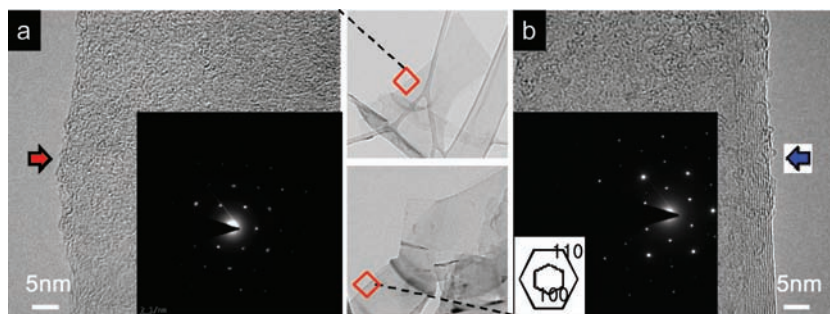


Figure 2. TEM images and diffraction peaks of graphene flakes. a) HRTEM image of single-layer graphene. No wrinkles are observed. b) HRTEM image of multilayer graphene. Many wrinkles are detected. Inset: diffraction pattern by TEM. If graphene is a single layer, the innermost diffraction spots from the (100) planes are brighter than the second innermost spots from the (110) planes.

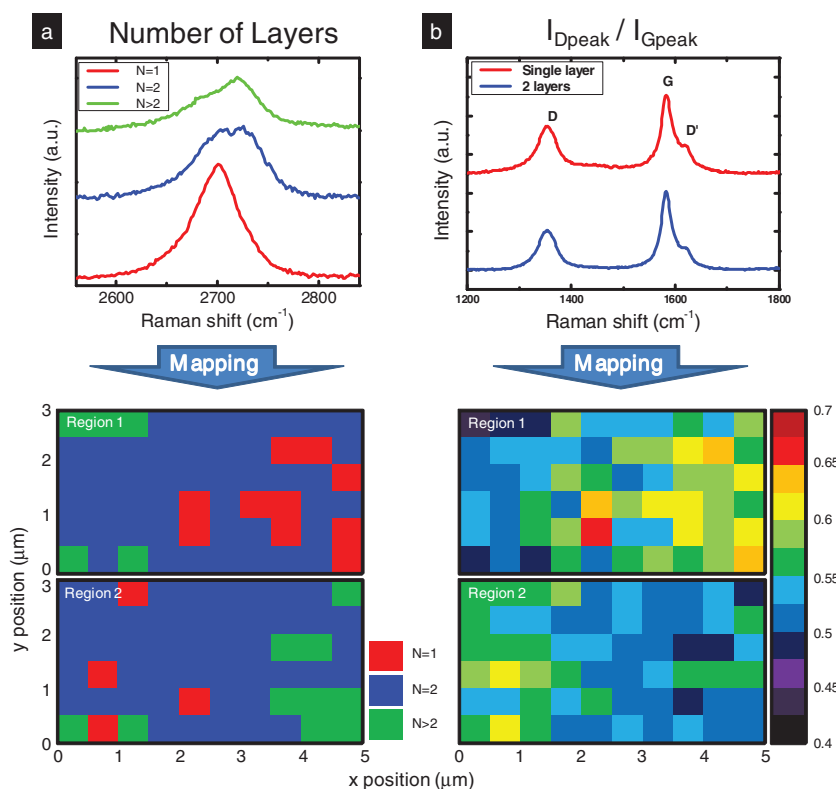


Figure 3. Raman mapping analysis in two regions of a graphene sheet centrifuged at 8000 g for 30 min. Size of each region is $5 \mu\text{m} \times 3 \mu\text{m}$. Raman laser whose spot size is $1 \mu\text{m} \times 1 \mu\text{m}$ is moved by 500 nm. a) Analysis of the number of layers by considering the shape of the **2D** peak. b) Intensity ratio, $I_{\text{Dpeak}}/I_{\text{Gpeak}}$.

Raman spectroscopy is a well-known indicator to determine the precise number of graphene layers.^[35] To confirm relations between the shape of **2D** peak and the number of graphene layers in our graphene flakes, we performed simultaneously atomic force microscopy (AFM) and Raman spectroscopy analysis. Figure S3a in the SI shows an AFM topography image of prepared graphene flakes and their measured heights. Figure S3b (SI) is the result of Raman spectroscopy on the flakes. From these results, the correlation between the shape of the **2D** peak and the number of graphene layers produced by this method becomes clear; the shape of the **2D** peak reveals that the flakes are bilayer graphene, and the measured height of -0.85 nm is in agreement with this finding. The above graph of Figure 3a (and Figure S3c, SI) presents a series of representative **2D** peak shapes measured from the produced graphene according to the number of layers. Because bilayer graphene has a much broader and up-shifted **2D** band compared to single-layer graphene, the **2D** peak analysis can easily distinguish single-layer graphene from the bi- or few-layer graphene produced in this work. Figure 3a is the corresponding mapping image, illustrating the number of graphene layers at given locations. The overall amount of single- or bi-layer graphene is above 80% in the sheets. In Figure 3b, the average **D** to **G** intensity ratio of single-layer graphene is 0.549, which is about half of the value achieved from reduced graphene.^[36] A smaller ratio of $I_{\text{Dpeak}}/I_{\text{Gpeak}}$ in Raman spectroscopy can be an important index to predict the quality of graphene,

because the **D** peak mostly originates from defects of graphene. Furthermore, two main reasons that increase the **D** peak intensity could be basal defects in the sp^2 network and edge defects of the graphene flakes. The contribution from the latter will be dominant as the flake size becomes smaller. Considering the small size of our flakes, the small value of the **D** to **G** ratio may prove the low defect density in the basal plane of graphene flakes.^[9,37] From this ratio, the prepared graphene has significantly less defects, thus promising better material properties, compared to flakes prepared from the conventional oxidation method. The above full plot of Figure 3b is used for the analysis. It is worth noting that a smaller number of layers is associated with a smaller $I_{\text{Dpeak}}/I_{\text{Gpeak}}$ ratio in general.

Although Hummers' method is an easy, low-cost process applicable to mass production, the conduction properties of the achieved graphene flakes is significantly worse than that of pristine graphene because residual oxygen atoms disrupt the graphene network and serve as scattering centers for electronic conduction. In this sense, stable methods for synthesizing graphene flakes with minimum oxidation are necessary.

Figure 4a is a plot of wide-scanning X-ray photoelectron spectroscopy (XPS) results. Graphene flakes prepared by our method have a high carbon peak and extremely low oxygen peak ($<2\%$) compared to those by Hummers' method. A detailed analysis of the carbon peak through narrow scanning and peak decompositions (Figure 4b) verifies that the final graphene flakes undergo very little oxidation from the original graphite source (SP-1 graphite, Bay Carbon) even after all the processing steps. The C–C bonding peak of graphene flakes (black line) remains unchanged from that of the graphite source (red dotted line) and the peak from C–O bonding (blue dotted line) is nearly negligible. Traceable amounts of potassium, chlorine, or iodine are not found from a further analysis of XPS peaks (Figure S4 in the SI).

Dispersed graphene flakes can be useful for many applications, especially for transparent and flexible electrodes.^[38,39] The dispersed graphene solution produced in this work can be of practical use for making large-area, low-cost transparent electrodes through a solution process. However, the dissolved salts in the solution need to be purified. To verify the possibility of application to transparent electrodes, the solution was first filtered by an aluminum oxide membrane filter with $0.1 \mu\text{m}$ pores (Whatman) and washed three times with 1,2-DCB and ethanol. After full drying in a vacuum oven at $80 \text{ }^\circ\text{C}$, the anodic aluminum oxide (AAO) filter was etched by NaOH; and to remove the NaOH residue of the film, it went through dilution by DI

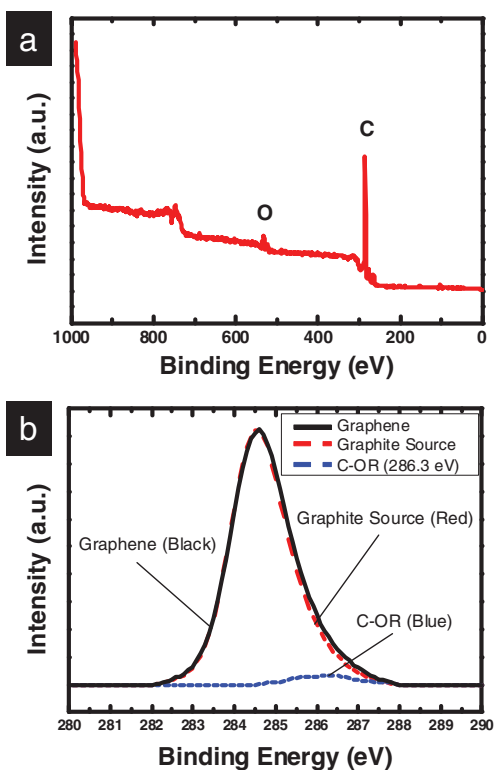


Figure 4. Oxygen analysis results by wide-scanned XPS (a) and narrow-scanned XPS in the oxide region (b).

water. The film was transferred to a polyethyleneterephthalate (PET) plastic substrate after etching the AAO filter. The film on the PET plastic substrate was annealed at 150 °C under H₂ atmosphere for 1 h. (**Figure 5a**) Because most plastic films are deformed or damaged above ~150–200 °C,

a low annealing temperature is a key processing condition for flexible electronics. As shown in **Figure 5b**, the film is transparent and flexible. The successive sheet surface was observed using scanning electron microscopy (SEM; inset of **Figure 5b**). Conductivity can be calculated from sheet resistance through a four-point probe measurement and the thickness of the graphene sheet. The conductivity of the transparent film is 11 033 S m⁻¹ (**Figure 5c**). The best conductivity of reduced graphene oxide film annealed below 150 °C is smaller than 8500 S m⁻¹ [9,21,40] even after complex reduction processes.^[21] Considering the low content of oxygen and the low **D** peak measured from Raman spectroscopy however, we believe that the conductivity of our sample can be significantly improved with further research. The suggested routes to achieve this are i) increasing the average size of the graphene flakes, which reduces the number of resistive contacts between flakes in the same conducting path length;^[9] ii) minimizing possible damage from the etching process of the AAO filter; and iii) improving the transfer process from the AAO filter to other substrates.

In conclusion, metal salts are promising intercalation agents to obtain metal-GICs and to exfoliate graphite in a simple, low-cost process. The proposed process produces high-quality graphene flakes (verified by TEM, Raman, and XPS analyses) in solvent, which is of great use in large-area applications with a solution process. The conductivity of our sample exceeds the highest conductivity reported to date for reduced graphene annealed below 150 °C. Since the use of KI is economically viable and allows ease of handling, the proposed method may become an alternative to the graphite oxidation and reduction method. Further experimental and theoretical work is necessary, however, to achieve optimized material properties (i.e., larger average size of graphene flakes).

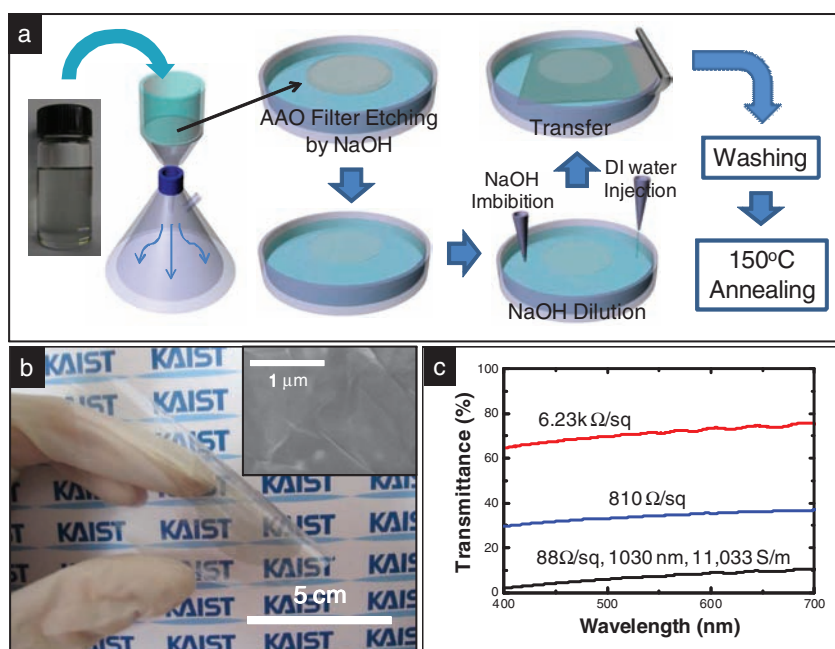


Figure 5. a) Schematic illustration of graphene sheet forming process. b) Transferred graphene sheet on PET film. Inset: SEM Image of the graphene sheet surface. c) Transmittance analysis of the graphene sheet.

Supporting Information

Supporting Information is available from the Wiley Online Library or from the author.

Acknowledgements

This research was supported by WCU (World Class University) program through the National Research Foundation of Korea funded by the Ministry of Education, Science and Technology (R32-10051), the National Research Foundation of Korea (NRF) funded by the Ministry of Education, Science and Technology (No. 2009-0083380), and Basic Science Research Program through the National Research Foundation of Korea (NRF) funded by the Ministry of Education, Science and Technology (CAFD-2010009890).

- [1] K. S. Novoselov, A. K. Geim, S. V. Morozov, D. Jiang, M. I. Katsnelson, I. V. Grigorieva, S. V. Dubonos, A. A. Firsov, *Nature* **2005**, *438*, 197.
- [2] Y. B. Zhang, Y. W. Tan, H. L. Stormer, P. Kim, *Nature* **2005**, *438*, 201.
- [3] C. Lee, X. D. Wei, J. W. Kysar, J. Hone, *Science* **2008**, *321*, 385.
- [4] A. K. Geim, *Science* **2009**, *324*, 1530.
- [5] M. J. Allen, V. C. Tung, R. B. Kaner, *Chem. Rev.* **2010**, *110*, 132.
- [6] C. Valles, C. Drummond, H. Saadaoui, C. A. Furtado, M. He, O. Roubeau, L. Ortolani, M. Monthieux, A. Penicaud, *J. Am. Chem. Soc.* **2008**, *130*, 15802.
- [7] J. H. Lee, D. W. Shin, V. G. Makotchenko, A. S. Nazarov, V. E. Fedorov, Y. H. Kim, J. Y. Choi, J. M. Kim, J. B. Yoo, *Adv. Mater.* **2009**, *21*, 4383.
- [8] S. Park, R. S. Ruoff, *Nat. Nanotechnol.* **2009**, *4*, 217.
- [9] U. Khan, A. O'Neill, M. Lotya, S. De, J. N. Coleman, *Small* **2010**, *6*, 864.
- [10] J. H. Lee, D. W. Shin, V. G. Makotchenko, A. S. Nazarov, V. E. Fedorov, J. H. Yoo, S. M. Yu, J. Y. Choi, J. M. Kim, J. B. Yoo, *Small* **2010**, *6*, 58.
- [11] C. Berger, Z. M. Song, X. B. Li, X. S. Wu, N. Brown, C. Naud, D. Mayou, T. B. Li, J. Hass, A. N. Marchenkov, E. H. Conrad, P. N. First, W. A. de Heer, *Science* **2006**, *312*, 1191.
- [12] S. Y. Zhou, G. H. Gweon, A. V. Fedorov, P. N. First, W. A. De Heer, D. H. Lee, F. Guinea, A. H. C. Neto, A. Lanzara, *Nat. Mater.* **2007**, *6*, 770.
- [13] K. S. Kim, Y. Zhao, H. Jang, S. Y. Lee, J. M. Kim, J. H. Ahn, P. Kim, J. Y. Choi, B. H. Hong, *Nature* **2009**, *457*, 706.
- [14] S. Y. Kwon, C. V. Ciobanu, V. Petrova, V. B. Shenoy, J. Bareno, V. Gambin, I. Petrov, S. Kodambaka, *Nano Lett.* **2009**, *9*, 3985.
- [15] X. S. Li, W. W. Cai, J. H. An, S. Kim, J. Nah, D. X. Yang, R. Piner, A. Velamakanni, I. Jung, E. Tutuc, S. K. Banerjee, L. Colombo, R. S. Ruoff, *Science* **2009**, *324*, 1312.
- [16] A. Reina, X. T. Jia, J. Ho, D. Nezich, H. B. Son, V. Bulovic, M. S. Dresselhaus, J. Kong, *Nano Lett.* **2009**, *9*, 30.
- [17] J. T. Robinson, F. K. Perkins, E. S. Snow, Z. Q. Wei, P. E. Sheehan, *Nano Lett.* **2008**, *8*, 3137.
- [18] M. D. Stoller, S. J. Park, Y. W. Zhu, J. H. An, R. S. Ruoff, *Nano Lett.* **2008**, *8*, 3498.
- [19] J. J. Liang, Y. Wang, Y. Huang, Y. F. Ma, Z. F. Liu, F. M. Cai, C. D. Zhang, H. J. Gao, Y. S. Chen, *Carbon* **2009**, *47*, 922.
- [20] W. S. Hummers Jr., R. E. Offeman, *J. Am. Chem. Soc.* **1958**, *80*, 1339.
- [21] D. R. Dreyer, S. Park, C. W. Bielawski, R. S. Ruoff, *Chem. Soc. Rev.* **2010**, *39*, 228.
- [22] B. Scrosati, *J. Electrochem. Soc.* **1992**, *139*, 2776.
- [23] M. S. Whittingham, *Chem. Rev.* **2004**, *104*, 4271.
- [24] A. Charlier, M. F. Charlier, D. Fristot, *J. Phys. Chem. Solids* **1989**, *50*, 987.
- [25] L. M. Viculis, J. J. Mack, O. M. Mayer, H. T. Hahn, R. B. Kaner, *J. Mater. Chem.* **2005**, *15*, 974.
- [26] H. K. Jeong, Y. P. Lee, R. Lahaye, M. H. Park, K. H. An, I. J. Kim, C. W. Yang, C. Y. Park, R. S. Ruoff, Y. H. Lee, *J. Am. Chem. Soc.* **2008**, *130*, 1362.
- [27] M. S. Dresselhaus, G. Dresselhaus, *Adv. Phys.* **2002**, *51*, 1.
- [28] D. W. McKee, *Carbon* **1979**, *17*, 419.
- [29] H. Marsh, D. S. Yan, T. M. Ogrady, A. Wennerberg, *Carbon* **1984**, *22*, 603.
- [30] C. E. Hamilton, J. R. Lomeda, Z. Z. Sun, J. M. Tour, A. R. Barron, *Nano Lett.* **2009**, *9*, 3460.
- [31] J. C. Meyer, A. K. Geim, M. I. Katsnelson, K. S. Novoselov, T. J. Booth, S. Roth, *Nature* **2007**, *446*, 60.
- [32] S. Horiuchi, T. Gotou, M. Fujiwara, R. Sotoaka, M. Hirata, K. Kimoto, T. Asaka, T. Yokosawa, Y. Matsui, K. Watanabe, M. Sekita, *Jpn J. Appl. Phys. 2 Lett.* **2003**, *42*, L1073.
- [33] Y. Hernandez, V. Nicolosi, M. Lotya, F. M. Blighe, Z. Y. Sun, S. De, I. T. McGovern, B. Holland, M. Byrne, Y. K. Gun'ko, J. J. Boland, P. Niraj, G. Duesberg, S. Krishnamurthy, R. Goodhue, J. Hutchison, V. Scardaci, A. C. Ferrari, J. N. Coleman, *Nat. Nanotechnol.* **2008**, *3*, 563.
- [34] A. Bagri, C. Mattevi, M. Acik, Y. J. Chabal, M. Chhowalla, V. B. Shenoy, *Nat. Chem.* **2010**, *2*, 581.
- [35] A. C. Ferrari, J. C. Meyer, V. Scardaci, C. Casiraghi, M. Lazzeri, F. Mauri, S. Piscanec, D. Jiang, K. S. Novoselov, S. Roth, A. K. Geim, *Phys. Rev. Lett.* **2006**, *97*, 187401.
- [36] H. L. Wang, J. T. Robinson, X. L. Li, H. J. Dai, *J. Am. Chem. Soc.* **2009**, *131*, 9910.
- [37] L. G. Cancado, K. Takai, T. Enoki, M. Endo, Y. A. Kim, H. Mizusaki, A. Jorio, L. N. Coelho, R. Magalhaes-Paniago, M. A. Pimenta, *Appl. Phys. Lett.* **2006**, *88*, 163106.
- [38] D. A. Dikin, S. Stankovich, E. J. Zimney, R. D. Piner, G. H. B. Dommett, G. Evmenenko, S. T. Nguyen, R. S. Ruoff, *Nature* **2007**, *448*, 457.
- [39] J. A. Rogers, *Nat. Nanotechnol.* **2008**, *3*, 254.
- [40] I. K. Moon, J. Lee, R. S. Ruoff, H. Lee, *Nat. Commun.* **2010**, *1*, 73.

Received: November 8, 2010
Revised: December 22, 2010
Published online: February 25, 2011